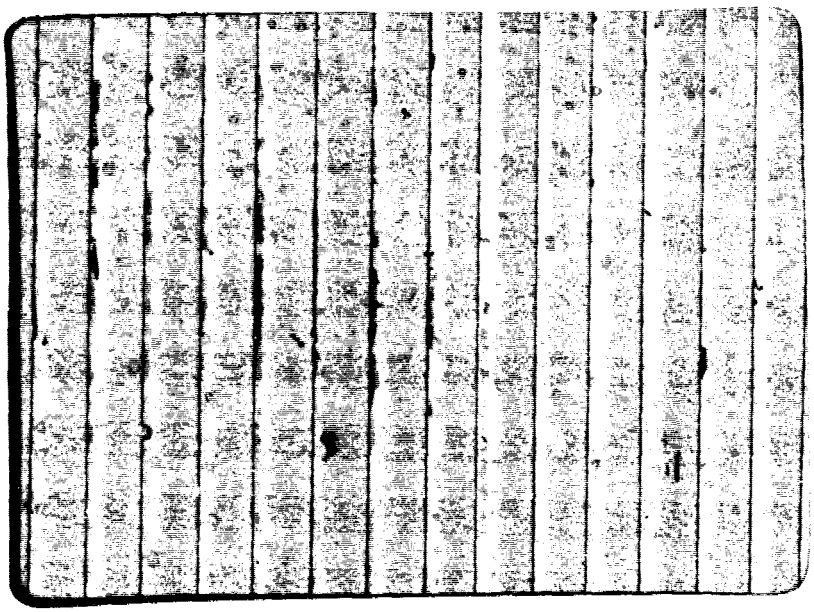

CONSELHO NACIONAL DE DESENVOLVIMENTO CIENTÍFICO E TECNOLÓGICO
INSTITUTO DE PESQUISAS ESPACIAIS

1.Classification *INPE-COM.10/PE* *C.D.U.: 523.035.1*	2.Period	4.Distribution Criterion internal ☐ external X
3.Key Words (selected by the author) *MEDIUM ENERGY GAMMA-RAYS* *ENERGY SPECTRUM OF GAMMA-RAYS*		
5.Report NQ *INPE-1218-PE/122*	6.Date *April, 1978*	7.Revised by *Inácio M. Martin*
8. Title and Sub-title *ENERGY SPECTRUM OF MEDIUM ENERGY GAMMA-RAYS FROM THE GALACTIC CENTER REGION*		9.Authorized by *Nelson de Jesus Parada* *Director*
10.Sector *DCE/DAS* Code *360*		11.NQ of Copies *21*
12.Authorship *R.A.R. Palmeira* *K. Ramanuja Rao* *S.L.G. Dutra* *D.L. Bertsch* *D.A. Kniffen* *D.J. Morris* 13.Signature of the responsible		14.NQ of Pages *23* 15.Price

16.Summary/Notes

Two balloon-borne experiments were performed in November and December 1975, at Southern latitude of 23° (Resende, Rio de Janeiro). In this paper, preliminary results of the second balloon flight, on December 3, are presented. The detector used was a digitized spark-chamber with 12 MeV minimum energy. The gamma-ray counting rate is given when the balloon is ascending and is at ceiling, to show the detection of galactic gamma-rays. The results clearly indicate the presence of diffuse component in this energy range.

17.Remarks *This work was partially supported by the "Fundo Nacional de Desenvolvimento Científico e Tecnológico - FNDCT", Brazil, under contract FINEP-CT/271.*

INDEX

ENERGY SPECTRUM OF MEDIUM ENERGY GAMMA-RAYS FROM THE GALACTIC CENTER REGION

by

R. A. R. Palmeira, K. Ramanuja Rao, S.L.G. Dutra

Instituto de Pesquisas Espaciais - INPE

Conselho Nacional de Desenvolvimento Científico e Tecnológico - CNPq

São José dos Campos - SP - Brasil

D.L. Bertsch, D.A. Kniffen

NASA, Goddard Space Flight Center, Greenbelt, USA

D.J. Morris

University of Maryland, College Park, USA

ABSTRACT

Two balloon-borne experiments were performed in November and December 1975, at Southern latitude of 23° (Resende, Rio de Janeiro). In this paper, preliminary results of the second balloon flight, on December 3, are presented. The detector used was a digitized spark-chamber with 12 MeV minimum energy. The gamma-ray counting rate is given when the balloon is ascending and is at ceiling, to show the detection of galactic gamma-rays. The results clearly indicate the presence of a diffuse component in this energy range.

RESUMO

Dois vôos de balão estratosféricos foram efetuados em novembro e dezembro de 1975, lançados de Resende, Rio de Janeiro, com latitude 23° Sul. Serão apresentados resultados preliminares do segundo vôo, em 03 de dezembro. O detector usado é uma câmara de centelha digitalizada, com uma energia mínima de 12 MeV. Uma curva de crescimento da contagem de raios gama durante a subida (e quando no teto) do balão será apresentada para estabelecer o fato de que raios gama extraterrestres estão sendo detectados. Claramente, os resultados indicam a presença de uma componente difusa, nesta faixa de energia.

1. INTRODUCTION

Through gamma-ray astronomy one can obtain observational evidence on many of the current problems in astrophysics, such as the end result of the evolutionary process in stars, the synthesis of elements in nature, the origin of the energetic cosmic rays and the dynamic, high energy processes in our galaxy and the universe. The great penetrating power of gamma-rays makes them a very valuable probe of the cosmic ray and matter distributions throughout the extent of the galaxy. The first positive results of celestial gamma-rays were obtained by Kraushar et al. (1972) from the satellite experiment flown on OSO-III, which clearly showed the emission of gamma-rays, with energies above 50 MeV, from the galactic disk. The recent results from the satellite experiments on SAS-2 and COS-B (Fichtel, C.E. and Stecker, F.W. (1976)), in the range > 35 MeV, gave more detailed picture of the high energy gamma radiation from the galactic center and anti-center regions, and also showed the presence of a diffuse component of the celestial gamma-ray intensity in this energy range. The presence of such a component in the energy range between 1 and 10 MeV was also shown by many balloon borne experiments (Vedrenne et al. (1971), Golenetski et al. (1971), Schonfelder and Lichti (1974), Daniel et al. (1972)). Measurements of this radiation could provide information and constraints on theories involving extra-galactic cosmic-ray and matter densities, both at present and in the cosmological past, since a diffuse intensity probably originates outside the galaxy.

2. IMPORTANCE OF MEDIUM ENERGY GAMMA-RAY OBSERVATIONS

The medium energy range (10-50 MeV) of gamma-ray intensity is of interest because the electron processes (bremsstrahlung) are the predominant source of gamma-rays in this range, in contrast to the higher energy region where nuclear processes, like π^0 decay, are expected to be the main source of gamma-rays as shown by Kniffen et al (1977). Figure 1, taken from Stecker (1977), shows the gamma-ray differential production rates

due to Bremsstrahlung and Compton processes, as well as due to π^0 decay, at 10 kpc calculated for a total gas density of 1 atom per cm^3 and starlight radiation density of 0.44 eV cm^{-3} and clearly shows the importance of electron processes in this energy range. The dominance of bremsstrahlung mechanism in this energy range implies, as in the pion decay model at higher energies, that the gamma-ray distribution is strongly dependent on the distribution of the relevant interstellar gas and, thus, the medium energy gamma-rays reveal the presence of galactic cosmic ray electrons, in the same way that high energy gamma-rays reveal the distribution of the galactic nuclear cosmic-rays.

Moreover, the diffuse component is contaminated, at energies below 10 MeV, both by the celestial lines and induced gamma-ray emitters in the material in and around the detector and, at energies above 50 MeV, by a strong background of high latitude diffuse galactic gamma radiation. Thus the medium energy range is the cleanest window for observing the all-sky diffuse gamma-ray component.

Data are scarce in the very difficult medium gamma-ray range. The data from satellites OSO-III, SAS-2, COS-B pertain to high energy gamma-rays (> 35 MeV) and the data from balloons by Vedrenne et al.(1971), Golenetski et al.(1971), Daniel et al.(1972), Schönfelder and Lichti (1974) relate to gamma-ray energies below 10 MeV. In the medium energy range only a few data, i.e., balloon measurementes of Samimi, Share and Kinzer (1974) and those of Agrinier et al.(1973) are available. An experimental programme has been developed to fill this important gap in the galactic gamma-ray studies.

3. THE EXPERIMENT

The basic instrument is a magnetic core digitized spark-chamber with two assemblies of spark-chambers above and below the scintillation counters (Figure 2). The upper array consists of 16 spark-chamber modules interleaved with 15 aluminium pair production plates of thickness 0.0813 cm (0.009 radiation lengths). The separation

between plates is 1.41 cm. The active area of the spark-chamber is 50 cm x 50 cm. The lower assembly, below the scintillation plane, contains three plates and four grids with a separation of 5.66 cm. A Cerenkov counter is located below the lower assembly. A plastic anticoincidende dome is used to reject the charged particles.

The pair production interaction is used to convert, identify and measure the properties of the gamma-rays incident from the top of the detector. The pcm data are recorded on the ground and later converted to digital data tapes, processed on IBM 360, and an orthogonal X- and Y- view of the spark chamber is obtained. Figure 3 shows such a view. After a pair is formed, the remaining plates serve as scattering material for estimating the energy of the electrons.

This instrument was launched twice, balloon-borne, on November 19, and December 3, 1975, from Resende, Rio de Janeiro. The height reached by the balloons was 2.5-3 millibars, where two drift scans were obtained viewing the galactic Center.

For the data analysis, first the unambiguous gamma-ray events are selected from all those events which satisfy the trigger logic of the spark chamber. For this purpose, we require that the positron-electron pair should form a distinctive picture appearing as an inverted Y or V in at least one of the orthogonal views. The events which are not considered fall into two categories. The first of these includes all events which originate in the detector walls, rather than in the conversion plates. The majority of the remaining events are single track ones which may be electrons entering through the bottom of the detector, Compton electrons or very high energy, unresolved pairs. Gamma-ray energy calculations are based on the multiple scattering of the pair electrons in the aluminium plates, and the arrival directions are based on a weighted bisector method which weights the estimated direction toward the higher energy electron. From the arrival direction in telescope coordinates, the attitude data are used to transform the apparent direction of arrival of the ambient photon into any selected celestial coordinate system.

4. CALIBRATION OF THE INSTRUMENT

To interpret the data it is essential to understand the instrument response as a function of incident photon energy, arrival direction and position. The response of the spark-chamber has been calculated, using a very detailed Monte Carlo program which simulates all major elements of the detector and the pair production, Compton, collisional and radiative loss, and multiple scattering processes are built into the program. Figure 4 gives the efficiency of the detector for various energies, for vertical incidence, and Figure 5 gives the efficiency of the detector at 20 MeV and 50 MeV for various angles of incidence. Figura 6 is a graph showing the efficiency of the detector at various energies for various angles of incidence.

5. RESULTS

In this paper, preliminary results of the second balloon flight on December 3, 1975 are presented. Figure 7 shows the gamma-ray counting rate in relation with residual pressure, when the balloon is ascending and is at ceiling. Figure 8 shows the same data in more detail. If we assume that no residual atmospheric flux is present at zero residual atmospheric pressure, the growth curve of the gamma-ray intensity should be linear, up to about 20 mb, and show zero counting rate at the top of the atmosphere. The dotted line in Figure 8 is the least-square fit of all data from 50 mb to 20 mb, with constraint of zero intensity at the top of the atmosphere, and the full line gives the polinomial fit to the complete data. The excess counting rate above the least-square fit represents the background gamma-ray flux, which can be calculated by assuming a spectrum, if the geometric factor for an isotropic flux is known.

The excess counting rate at the top of the atmosphere is given by

$$N = \int_0^\infty G(E)\, J(E)\, dE$$

where G(E) is the geometrical factor including the efficiency of the detector and J(E) is the flux at energy E. The detector responds efficiently between 15 and 70 MeV and so the integral flux in this range is obtained as

$$J_{(15-70)} = \frac{N}{\int_{15}^{70} G(E)\, dE} = (5.2 \pm 0.5) \times 10^{-7}/(cm^2\text{-s-ster-MeV})$$

from the excess counts N = 3,4 counts/min at 3 millibars, as seen in Figure 8. As no distinction has been made between different energy ranges in these preliminary results, this integral flux is shown in Figure 9, along with other results, as a differential line, spread between 15 and 70 MeV, with an average energy of 28 MeV, obtained by assuming a spectral shape $E^{-2.2}$ for the residual flux and using the equation

$$\bar{E} = \frac{\int_{15}^{70} E \cdot E^{-2.2}\, dE}{\int_{15}^{70} E^{-2.2}\, dE}$$

6. DISCUSSION

The present results show a low background flux, compared to the results of Agrinier et al. (1973) and Kniffen et al. (1977), which were obtained at the same location as this experiment, the later results being from the first experiment from the present series. This is because the present results do not include the background flux from the galaxy, which was only about 20 degrees from the horizon when these were obtained. Moreover the results give an integral flux between 15 and 70 MeV compared to the differential

points in the other results. However, these results give evidence for the existence of a residual gamma-ray flux above 15 MeV at the top of the atmosphere. In Figure 9 is plotted the function $\frac{dJ}{dE} = 0.485\ E^{-3.13}$, which is a best fit curve to all the data between 10 and 100 MeV, including that from SAS-2 satellite. It is seen that this has a much steeper spectral shape compared to the function $\frac{dJ}{dE} = 0.011\ E^{-2.3}$ plotted by Fichtel et al. (1975) to pass through the high-energy X-ray data and the SAS-2 data. It is also observed from Figure 9, that the gamma-ray flux between 10 and 40 MeV is high compared to that obtained by the above function. However, the present results are much below the level of this function. Though, many theories have been proposed to explain the diffuse radiation; including the interaction of electrons with matter, photons or magnetic fields and the cosmological models, such as particle-antiparticle annihilation model, cosmic ray - intergalactic matter or black-body interaction model, the origin and nature of the diffuse gamma-ray intensity is still an open question. Kniffen et al. (1977), in extending the model developed to explain the high energy gamma-ray observations of SAS-2 (Fichtel et al. (1977)) to medium energy range, showed that the bremsstrahlung spectrum, shifted up by a factor of 3, reasonably fits the first balloon data in this series of experiments. Such a high bremsstrahlung contribution, in this energy range, is compatible with the predictions of Ramaty and Westergaard (1976) for the closed galaxy model. Other reasons for the higher intensity of diffuse gamma-ray flux in this region, giving the observed bulge in the spectrum as shown by other results between 10 and 40 MeV, may be either due to the contribution of galactic disk or due to a much higher local interstellar electron intensity.

7. SUMMARY

To measure the medium energy gamma-ray flux, two balloons were flown, with spark-chamber as the detector, at the Southern latitude of 23^0 (Resende, Rio de Janeiro). The preliminary results clearly indicate the presence of a diffuse component in this energy

range, in agreement with other observations in this region. As the medium energy gamma-rays reveal the presence of galactic cosmic ray electrons, in the same way as high-energy gamma-rays reveal the distribution of galactic nuclear cosmic rays, the observations in this energy range are important in understanding the distribution of interstellar gas and cosmic-ray densities, both at the present and in the cosmological past.

REFERENCES

Agrinier, B et al 1973 Proceedings of the 13th International Cosmic Ray Conference, 1, p. 8.

Bratolyubova et al 1971 Geomag. and Aeronomy, 11, p. 585.

Daniel et al 1972 Ap. and Space Sci., 18, p. 462.

Fichtel, C.E. et al 1975 Ap. J., 198, p. 163.

Fichtel, C.E. and Stecker, F.W. 1976 *Structure and Content of the Galaxy and galactic gamma rays*, NASA C.P. 002.

Fichtel, C.E. et al 1977 Proceedings of the 12th ESLAB Symposium, Frascati.

Galenetski et al 1971 Ap. Letters, 9, p. 69.

Herterich, W. et al 1973 Proceedings of the 13th International Cosmic Ray Conference, 1, p. 21.

Kniffen, D.A. et al 1977 Proceedings of the 12th ESLAB Symposium, Frascati. p. 117.

Kraushar, W.L. et al 1972 Ap. J., 177, p. 341.

Mayer-Hasselwander et al 1973 Ap. J. Letters, 175, L 23.

Ramaty, R. and Westergaard, N.J. 1976 Astr. Space Sci., 45, p. 143.

Samimi, J.; Share, G.H. and Kinzer, R.L. 1974 Proceedings of the 9th ESLAB Symposium, Frascati, p. 211.

Schönfelder and Lichti 1974 Ap. J. Letters, 191, L 1.

Stecker, F.W. 1977 Ap. J. 212, p. 60.

Vedrenne et al 1971 Astr. Astrophy. 15, p. 50.

FIGURE CAPTIONS

Figure 1: Local galactic γ-ray differential production rate for a total gas density of 1 atom per cm^3 and starlight radiation density of 0.44 eV cm^{-3}.

Figure 2: Medium energy 1/2 M x 1/2 M digitized spark chamber gamma ray telescope.

Figure 3: Computer reproduction of a gamma ray event in the spark chamber telescope.

Figure 4: Efficiency of spark chamber telescope at various energies for vertical incidence of gamma rays.

Figure 5: Efficiency of spark chamber telescope at 20 MeV and 50 MeV for various angles of incidence of gamma rays.

Figure 6: Efficiency of spark chamber telescope at various energies for various angles of incidence of gamma rays.

Figure 7: Gamma ray counting rate in relation with the residual pressure while the balloon is ascending.

Figure 8: Growth curve of gamma rays near the ceiling with a least square fit of all data from 50 mb to 20 mb.

Figure 9: Diffuse celestial gamma radiation observed by several experiments. The shaded area represents the SAS-2 data to-gether with its uncertainty. The line is the function $0.485\ E^{-3.13}$.

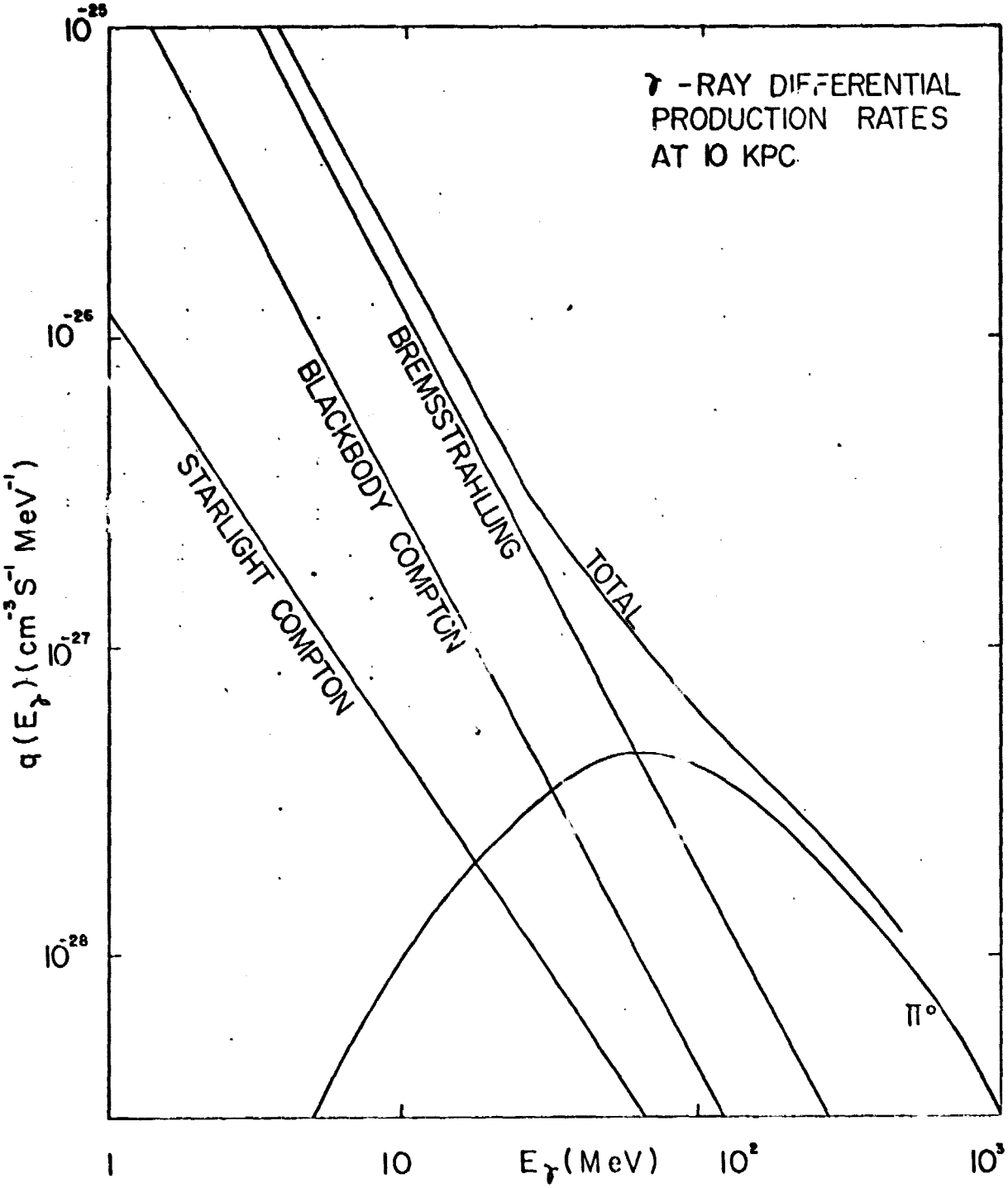

Fig. 1 - Local galactic γ-ray differential production rate for a total gas density of 1 atom per cm^3 and starlight radiation density of 0.44 cm^{-3}.

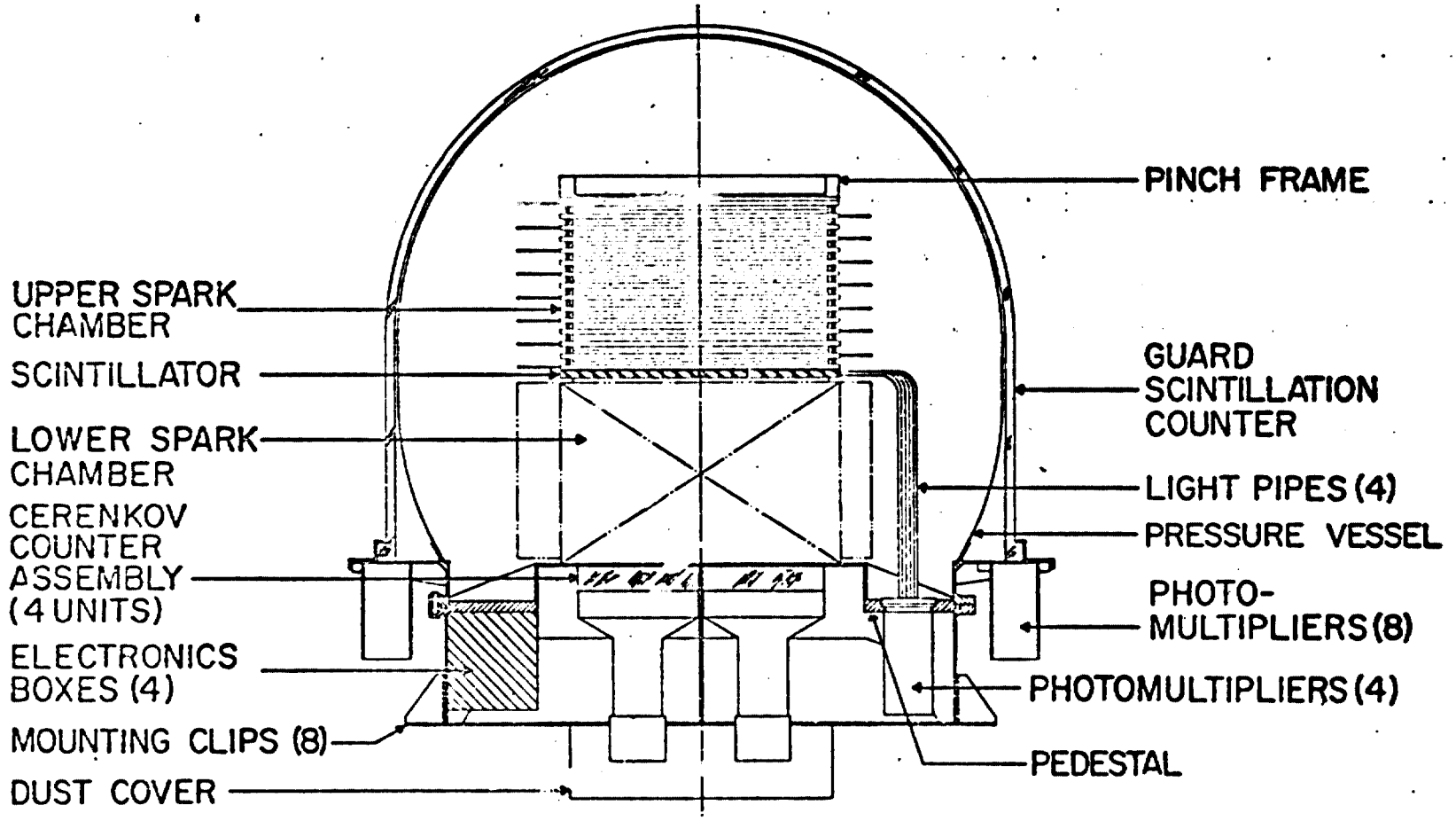

Fig. 2 - Medium energy 1/2 M x 1/2 M digitized spark chamber gamma ray telescope.

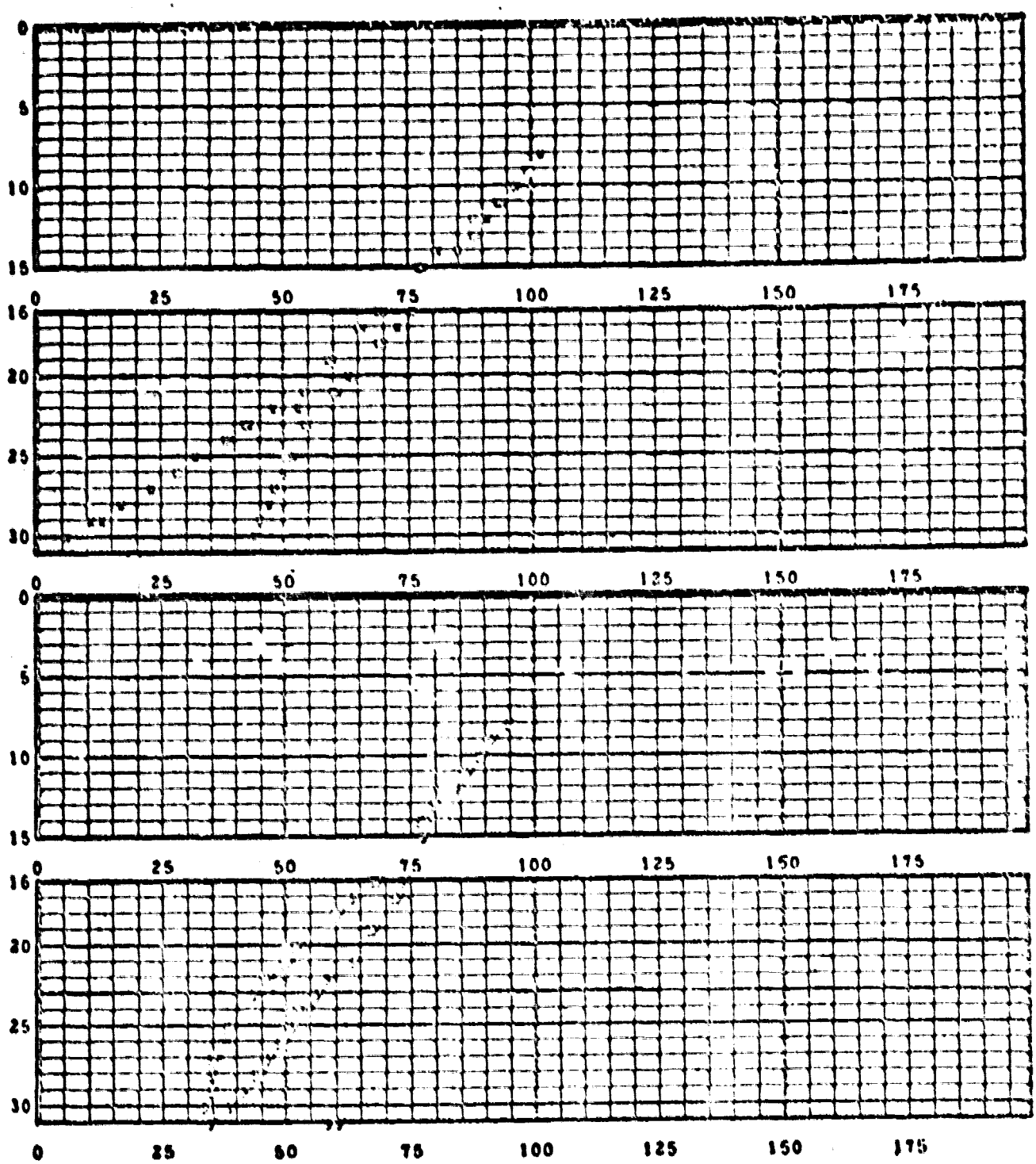

Fig. 3 - Computer reproduction of a gamma ray event in the spark chamber telescope

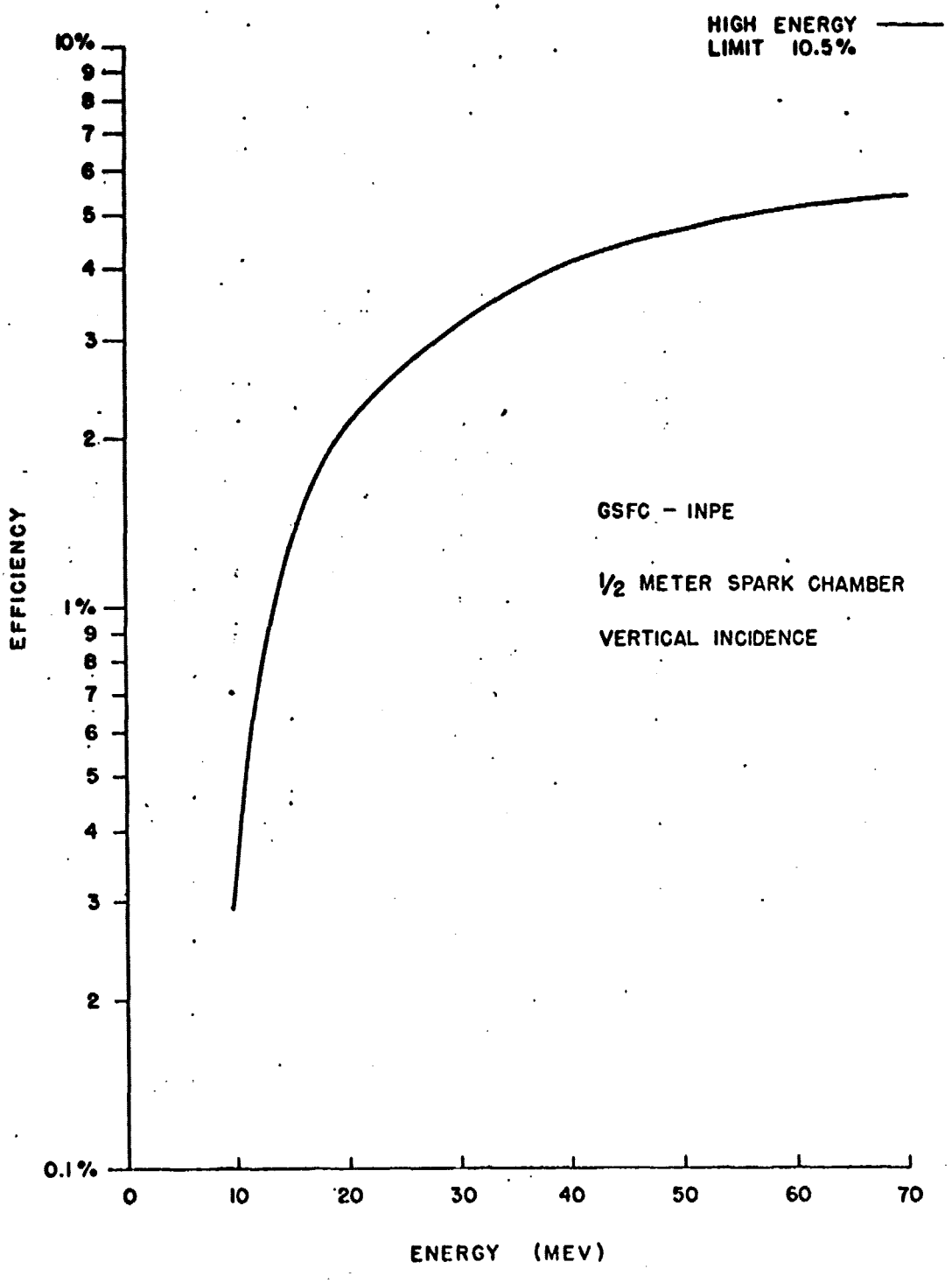

Fig. 4 - Efficiency of spark chamber telescope at various energies for vertical incidence of gamma rays

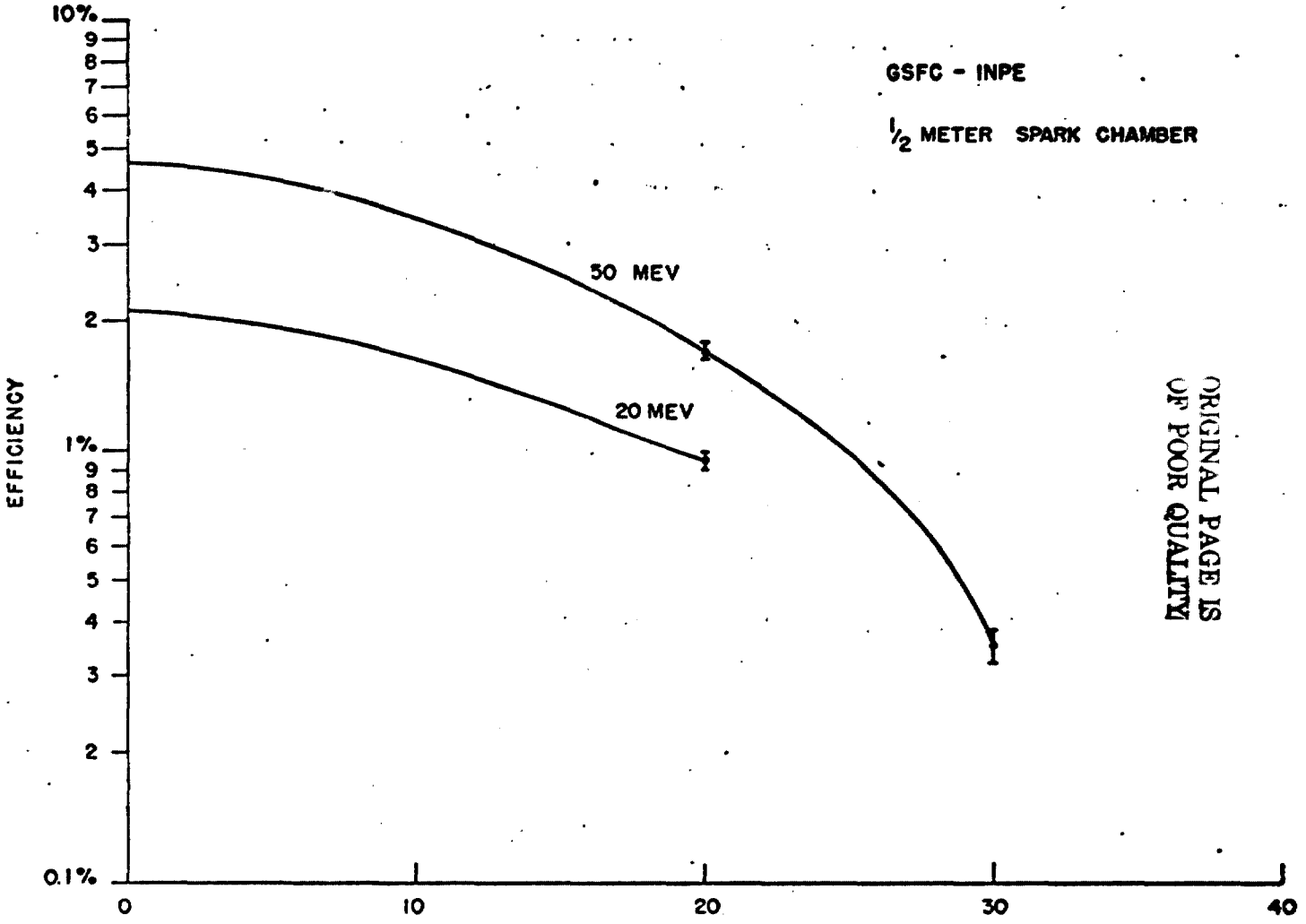

Fig. 5 - Efficiency of spark chamber telescope at 20 MeV and 50 MeV for various angles of incidence of gamma rays

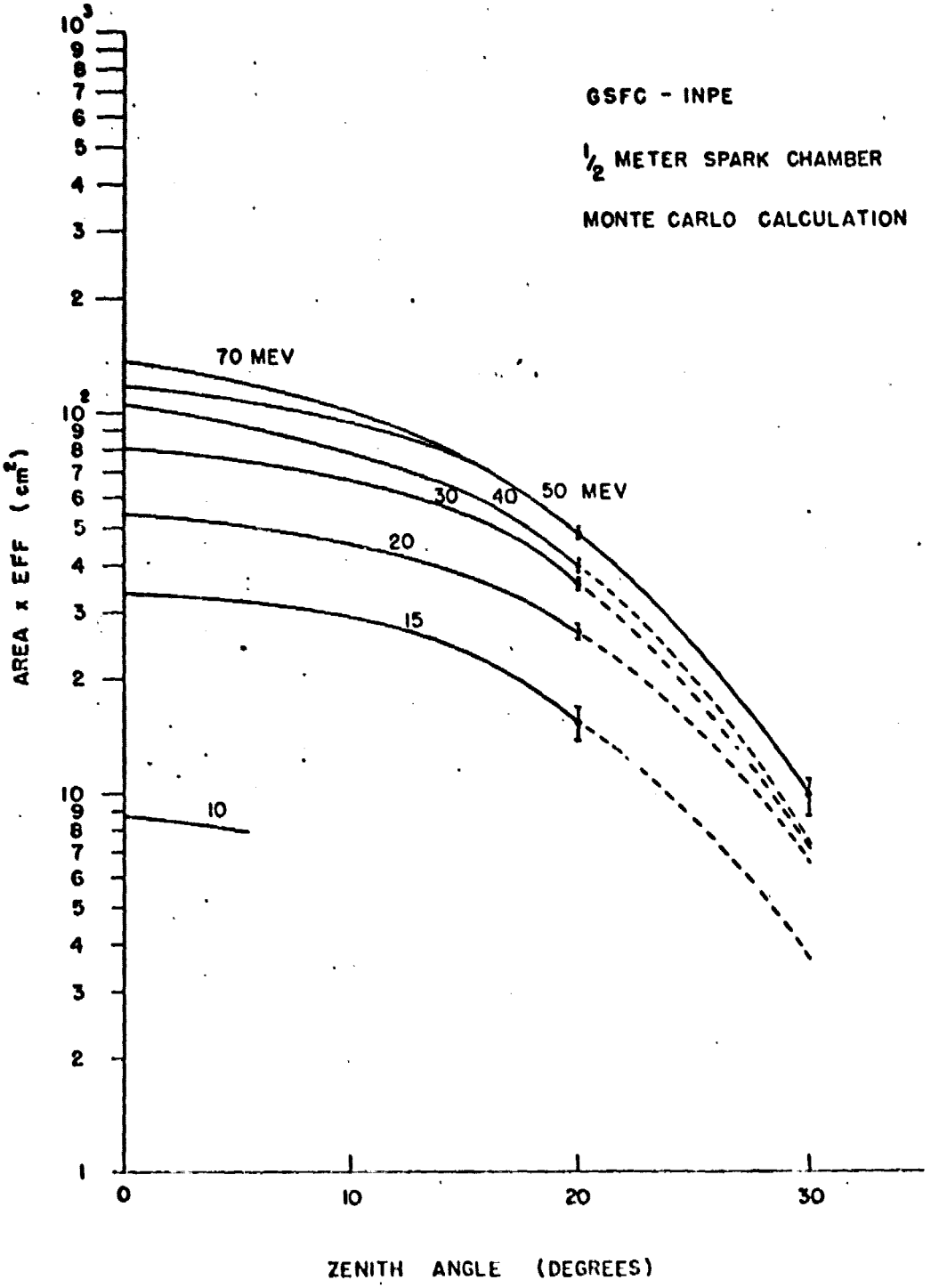

Fig. 6 - Efficiency of spark chamber telescope at various energies for various angles of incidence of gamma rays

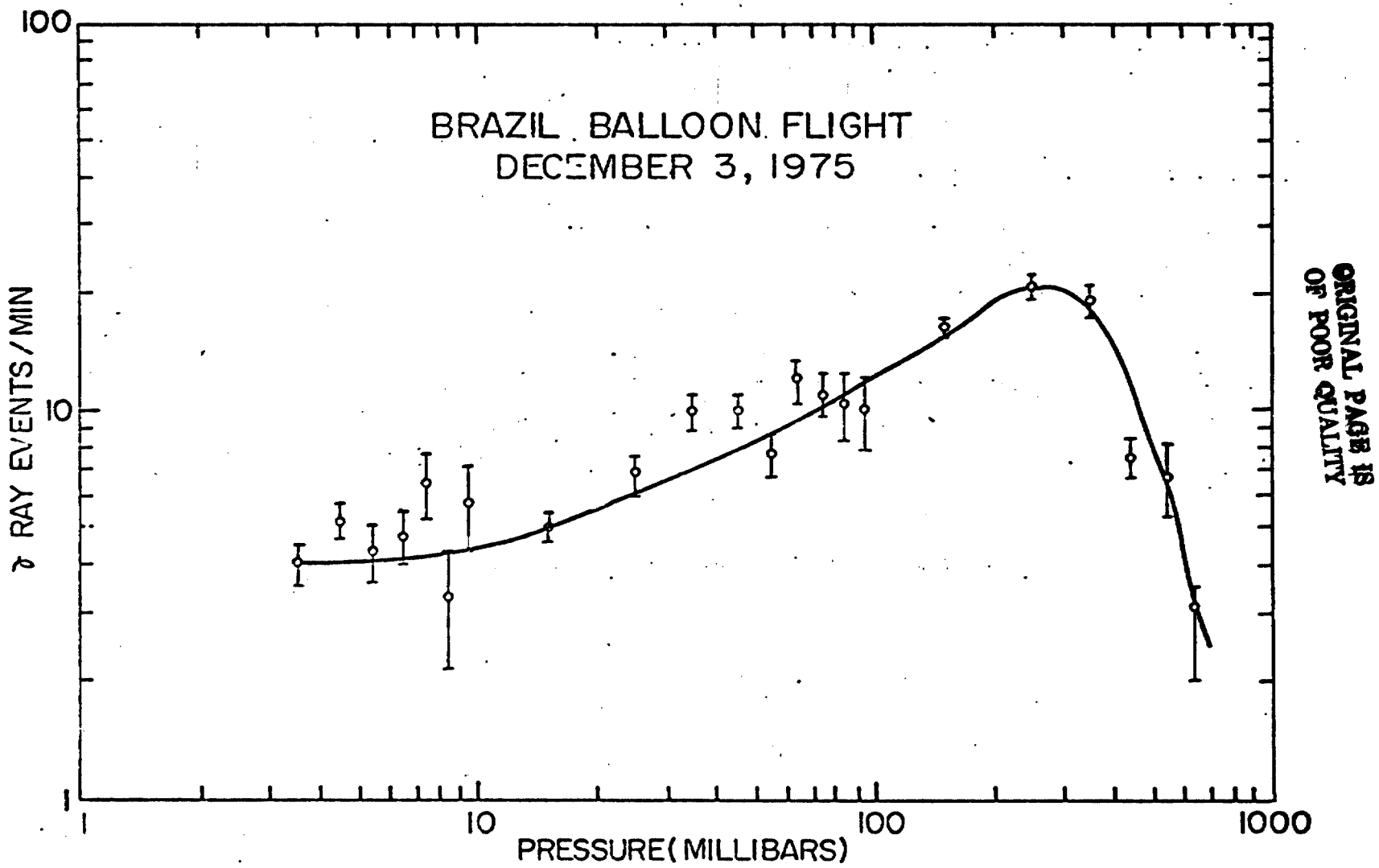

Fig. 7 - Gamma ray counting rate in relation with the residual pressure while the balloon is ascending

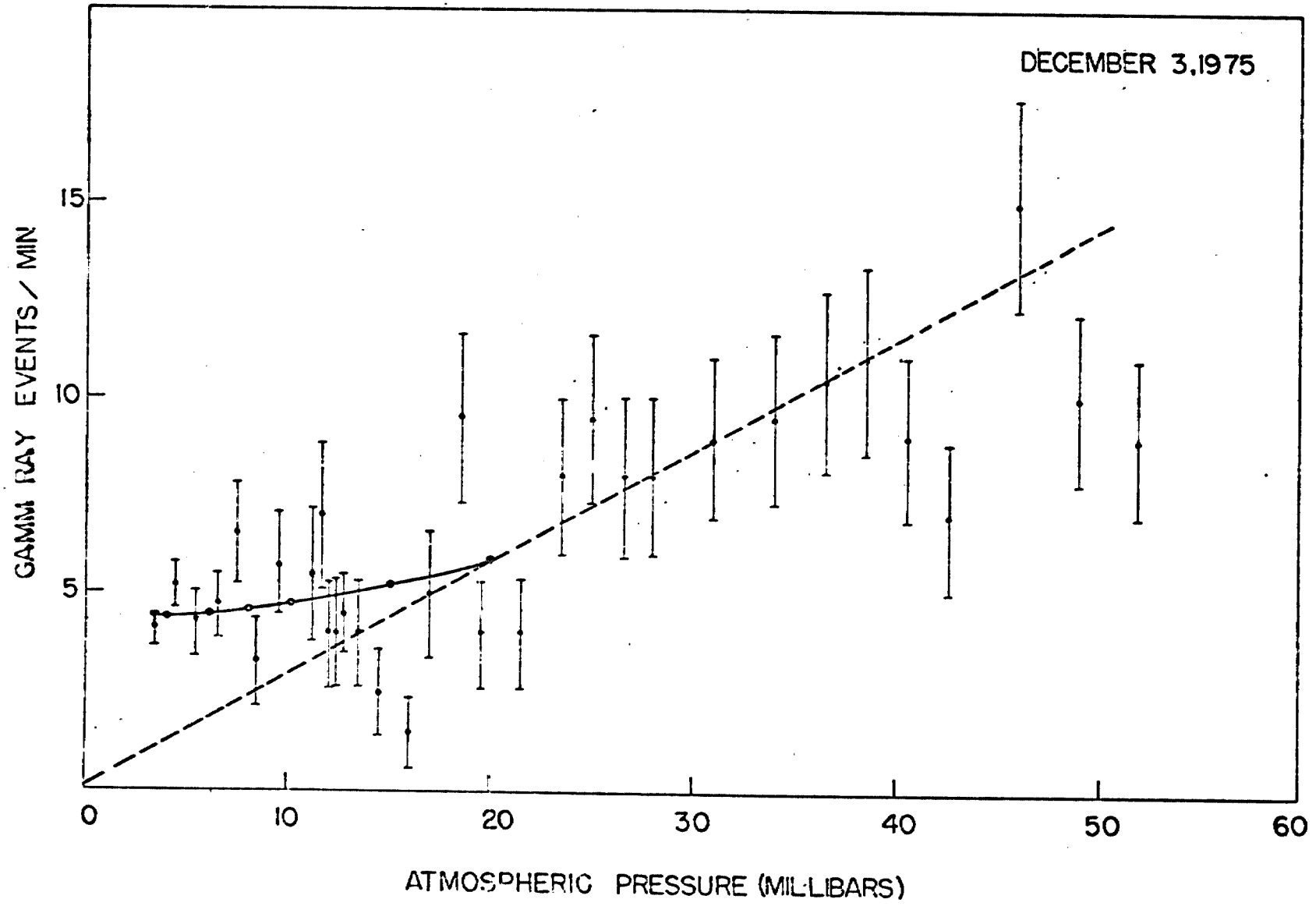

Fig. 8 - Growth curve of gamma rays near the ceiling with a least square fit of all data from 50 mb to 20 mb

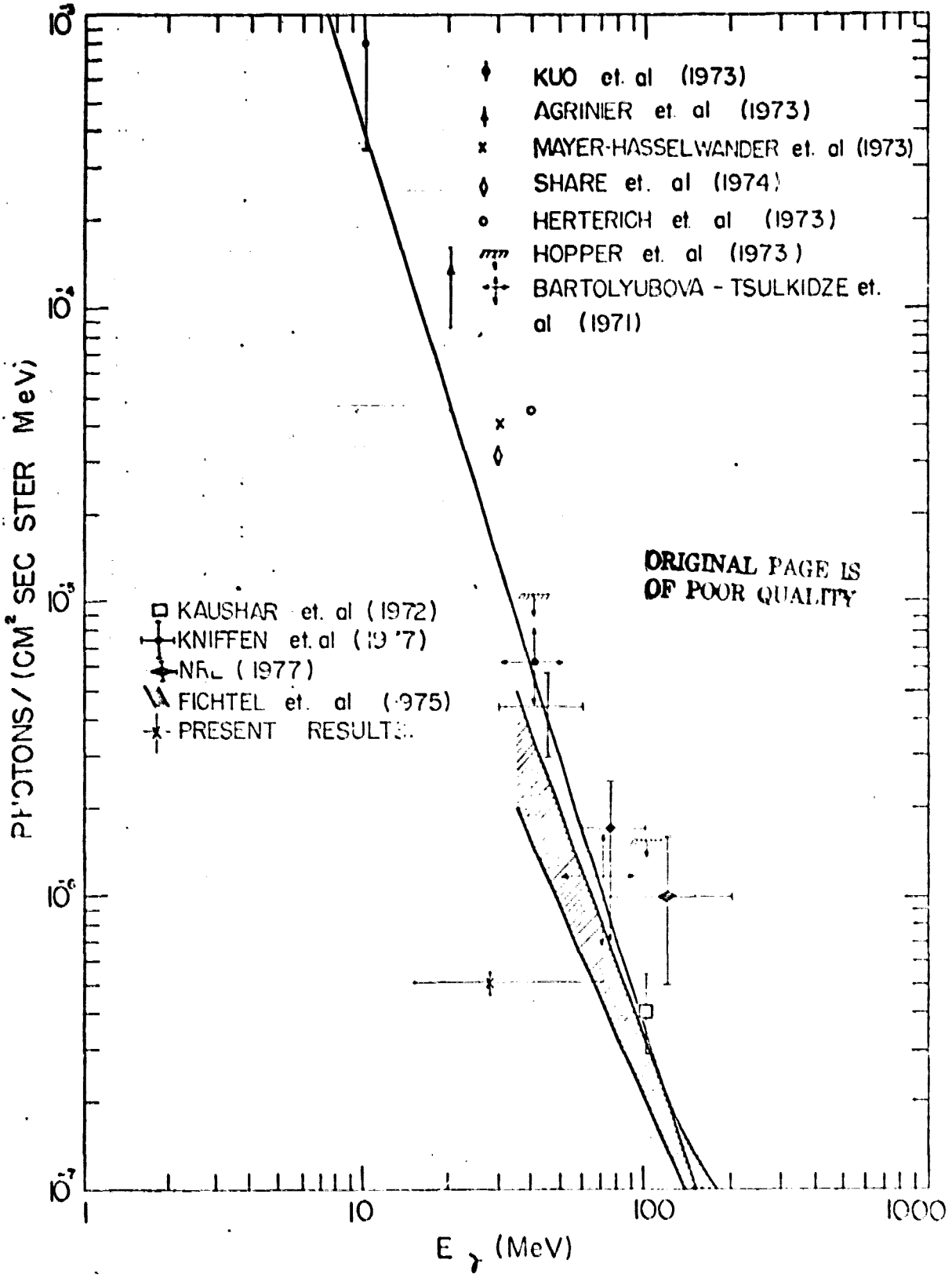

Fig. 9 - Diffuse celestial gamma radiation observed by several experiments. The shaded area represents the SAS-2 data together with its uncertainty. The line is the function $0.485\ E^{-3.13}$.